Science of the Total Environment 659 (2019) 587–598

Contents lists available at ScienceDirect

Science of the Total Environment

journal homepage: www.elsevier.com/locate/scitotenv

Massive tree mortality from flood pulse disturbances in Amazonian floodplain forests: The collateral effects of hydropower production

Angélica Faria de Resende [a,b,*], Jochen Schöngart [a], Annia Susin Streher [c], Jefferson Ferreira-Ferreira [c,d], Maria Teresa Fernandez Piedade [a], Thiago Sanna Freire Silva [c]

[a] National Institute of Amazonian Research (INPA), Coordination of Environmental Studies (CDAM), Av. André Araújo 2936, 69060-001 Manaus, Brazil
[b] National Institute for Amazonian Research (INPA), Av. André Araújo 2936, 69060-001 Manaus, Brazil
[c] Universidade Estadual Paulista (Unesp), Instituto de Geociências e Ciências Exatas, Ecosystem Dynamics Observatory, Avenida 24-A 1515, 13506-900 Rio Claro, Brazil
[d] Instituto de Desenvolvimento Sustentável Mamirauá, Estrada do Bexiga, 2584, Bairro Fonte Boa, Tefé, AM 69470-000, Brazil

HIGHLIGHTS

- Considerable floodplain forest loss occurred downstream of the Balbina dam from flood pulse changes;
- Several tree species are still suffering mortality, which may increase dead stand areas;
- Remote sensing methods used here may be applied to other floodplains with massive tree mortality by damming;
- Downstream igapó forests are highly sensitive to the loss of low water periods resulting from flow alteration by dam operations;

GRAPHICAL ABSTRACT

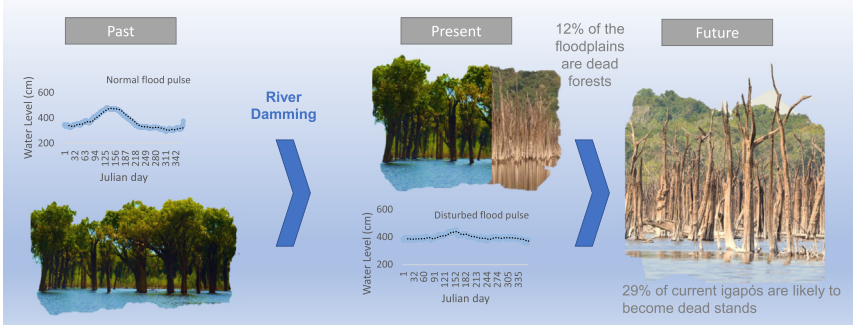

ARTICLE INFO

Article history:
Received 17 June 2018
Received in revised form 7 December 2018
Accepted 13 December 2018
Available online 15 December 2018

Editor: Ralf Ludwig

Keywords:
PALSAR
Synthetic aperture radar
Object-based image analysis
igapós
Black water river
Tree mortality
Hydropower dam

ABSTRACT

Large dams built for hydroelectric power generation alter the hydrology of rivers, attenuating the flood pulse downstream of the dam and impacting riparian and floodplain ecosystems. The present work mapped black-water floodplain forests (*igapó*) downstream of the Balbina Reservoir, which was created between 1983 and 1987 by damming the Uatumã River in the Central Amazon basin. We apply remote sensing methods to detect tree mortality resulting from hydrological changes, based on analysis of 56 ALOS/PALSAR synthetic aperture radar images acquired at different flood levels between 2006 and 2011. Our application of object-based image analysis (OBIA) methods and the random forests supervised classification algorithm yielded an overall accuracy of 87.2%. A total of 9800 km^2 of *igapó* forests were mapped along the entire river downstream of the dam, but forest mortality was only observed below the first 49 km downstream, after the Morena rapids, along an 80-km river stretch. In total, 12% of the floodplain forest died within this stretch. We also detected that 29% of the remaining living *igapó* forest may be presently undergoing mortality. Furthermore, this large loss does not include the entirety of lost *igapó* forests downstream of the dam; areas which are now above current maximum flooding heights are no longer floodable and do not show on our mapping but will likely transition over time to upland forest species composition and dynamics, also characteristic of *igapó* loss. Our results show that floodplain forests

* Corresponding author at: National Institute of Amazonian Research (INPA), Program of Post-Graduation in Botany, Coordination of Environmental Studies (CDAM), Av. André Araújo 2936, 69060-001 Manaus, Brazil.
E-mail address: gel.florestal@gmail.com (A.F. Resende).

https://doi.org/10.1016/j.scitotenv.2018.12.208

Balbina
Uatumã River
Amazon
Flood pulse

are extremely sensitive to long-term downstream hydrological changes and disturbances resulting from the disruption of the natural flood pulse. Brazilian hydropower regulations should require that Amazon dam operations ensure the simulation of the natural flood-pulse, despite losses in energy production, to preserve the integrity of floodplain forest ecosystems and to mitigate impacts for the riverine populations.

1. Introduction

Hydroelectric dams are a growing threat to the extensive Amazon wetlands, having several negative environmental effects and disturbing the hydrological balance that controls the structure and function of these environments (Castello and Macedo, 2016; Foote et al., 1996; Kahn et al., 2014; Latrubesse et al., 2017; Timpe and Kaplan, 2017). Although dams are important for electricity production, they also increase greenhouse gas emissions, disrupt indigenous and riverine communities, and lead to forest degradation and losses of biodiversity as a consequence of the large areas artificially inundated by the reservoirs behind storage dams (Benchimol and Peres, 2015; Cochrane et al., 2017; Fearnside, 1995; Junk and de Mello, 1990; Kemenes et al., 2007). Most ecological studies of hydropower dam impacts assess only the inundated and surrounding areas of reservoirs, while downstream environmental alterations caused by the hydrological changes created by dams remain poorly understood (Assahira et al., 2017; Manyari and de Carvalho, 2007; Timpe and Kaplan, 2017; Williams and Wolman, 1984).

Dams typically alter the natural "flood pulse" (Junk et al., 1989), negatively affecting the ecological dynamics of downstream floodplain ecosystems (Benchimol and Peres, 2015; Fearnside, 1995; Junk and Mello, 1990; Kemenes et al., 2007). Under natural conditions, the flood pulse of large rivers is predictable, characterized by a monomodal flood pulse with an annual cycle of rising, high, receding and low water phases, which can span more than 10 m of amplitude in the case of Central Amazonia (Junk et al., 2011; Schöngart and Junk, 2007). This natural water level oscillation floods over 750,000 km^2 annually in the Amazon Basin (Wittmann and Junk, 2017), varying in amplitude and duration depending on the amount and seasonality of rainfall within catchments, and on river discharge and topography (Junk et al., 2011). The flood pulse is the main driver of ecological and biogeochemical processes in floodplain forests (Junk, 1989; Lewis et al., 2000), where trees display anatomical, morphological, physiological, and biochemical adaptations to survive in this seasonal environment (De Simone et al., 2003; Ferreira and Parolin, 2011; Junk, 1989; Parolin et al., 2004). For this reason, a large number of tree species are endemic to floodplain environments (Wittmann et al., 2006, 2013, 2017).

Within the Amazonian floodplains, *igapós* are forests influenced by black or clear water (oligotrophic) rivers with catchments in the Precambrian Guiana shield and Central Brazilian archaic shield, receiving much lower sediment loads than the eutrophic *várzea* forests, which are inundated by sediment-rich white-water rivers with catchments in the Andean region (Junk et al., 2011; Prance, 1979; Sioli, 1984). Due to their low sediment load, black water and clear water rivers have been the main targets of hydroelectric projects across the Brazilian Amazon. Furthermore, several *igapó* areas along clear water rivers are close to the so-called "Arc of Deforestation", the expanding southwestern agricultural frontier in the Amazon, further compounding the threats to these systems (Lees et al., 2016).

Floodplain forest trees are recognized as good bioindicators of hydrological disturbances, due to their longevity (Schöngart et al., 2005). Many species have a seasonal growth pattern closely linked to the hydrological cycle (Schöngart et al., 2002), and changes in the regularity and duration of the natural flood cycle can lead to growth reduction or interruption and even to mortality. Assahira et al. (2017) found that a substantial increase in annual minimum water levels observed for several consecutive years in the Uatumã River, caused by water released from the Balbina Reservoir for power generation, led to the mortality of large populations of the highly flood-adapted tree species *Macrolobium acaciifolium* (Benth.) Benth. (Fabaceae) (Schlüter and Furch, 1992).

The number of hydroelectric power plants in the Amazon has grown steadily in the last 30 years, and this growth is expected to continue because these ventures are considered to be important for economic development, with efforts to understand and manage their socioecological implications often rushed and inadequate (Tilt, 2012; Tilt et al., 2009). Recent studies show conflicting data on the number of hydroelectric plants in operation, under construction and planned, even for papers published within the same year (Castello et al., 2013; Latrubesse et al., 2017; Lees et al., 2016; Timpe and Kaplan, 2017). Latrubesse et al. (2017) identified 140 dams in operation or under construction and 288 planned dams in the entire Amazon region. However, Anderson et al. (2018) reported 142 dams in operation or under construction and 160 planned dams for the Andean Amazon alone, implying a considerable underestimation from the remaining studies (Anderson et al., 2018; Castello and Macedo, 2016; Finer and Jenkins, 2012; Forsberg et al., 2017).

Disruptions in connectivity are also known to compromise the physical habitat and the ecological integrity of river systems around the world, threatening endemic species and allowing the colonization of invasive ones (Ligon et al., 1995; Mumba and Thompson, 2005; Nilsson, 2000; Ward and Stanford, 1995). In the case of large-scale Amazonian hydroelectric dams, existing studies have a very limited spatial distribution, and thus the true impacts and the extent of environmental disturbances caused by them remain only partially understood (Fearnside, 2014; Junk and Mello, 1990; Wittmann and Junk, 2017). There is a pressing need to quantify and understand the processes that occur downstream of Amazonian dams, where the natural flood pulse is completely altered by the opening and closing of floodgates, thereby altering the natural seasonality of the rivers (Assahira et al., 2017; Junk and Mello, 1990).

The construction of the Balbina Dam (Amazonas, state, Brazil) between 1983 and 1987 led to an abrupt change in the Uatumã River hydrology, which has been maintained for the past 30 years, providing an ideal system to assess ecohydrological responses to damming in *igapó* environments. Therefore, in the present study we address the following questions: (1) What is the spatial distribution and extent of tree mortality in *igapó* floodplain forests in the Uatumã River, downstream of the Balbina Dam? (2) Which recommendations can be made for future evaluations of environmental impacts of future hydroelectric dams in the Amazon region with focus on downstream areas? (3) Is *igapó* vegetation loss still occurring, and if so, in which areas?

2. Methods

2.1. Study area

We studied a 300-km stretch of the Uatumã River downstream of the Balbina hydroelectric dam, up to its confluence with the Amazon River, including major tributaries (Abacate and Jatapú rivers - see Fig. S1, showing the non-disturbed Abacate River *igapó*). The Uatumã River has a catchment area of approximately 69,500 km^2, corresponding to nearly 1.2% of the entire Amazon Basin (Melack and Hess, 2010).

The Balbina hydroelectric plant, built between 1983 and 1987, is known worldwide as one of the largest ecological disasters in Brazilian history (Fearnside, 1989). Its damming flooded about 4437 km^2 (Benchimol and Peres, 2015), but due to the low slope of the relief, the 250 MW of nominal energy produced is extremely low in relation to the flooded area. Compared to the Tucuruí hydroelectric dam on the Tocantins River, whose reservoir is nearly 100 km^2 smaller, the Balbina hydroelectric power plant produces almost 33 times less energy (International Rivers and ECOA, 2017).

Our study area is located approximately 150 km east of the capital city of Manaus (Amazonas state), within the Uatumã Sustainable Development Reserve (RDS Uatumã) (Fig. 1). Four distinct forest types are described for this region: upland forests (*terra firme*), oligotrophic floodplain forests (*igapó*), and two white-sand open vegetation (*campinas* and *campinaranas*) (Adeney et al., 2016; Andreae et al., 2015; IDESAM, 2009; Targhetta et al., 2015). According to data acquired between 2013 and 2015 from the Amazon Tall Tower Observatory (ATTO) project, the area has an average annual temperature of 27 °C and an average annual total rainfall of 1920 mm, with August and September being the driest months.

According to the Shuttle Radar Topography Mission (SRTM) global digital elevation model, the first 22 km of the Uatumã River downstream of the dam have an average width of 200 m (Figs. 1 and 2). For the next 13 km downstream, the river and its associated floodplain widen progressively, coinciding with a change from a rectilinear to a meandering pattern. The topographic profile from the dam to the Uatumã river mouth shows a steep descending gradient, with the steepest portions occurring up to 35 km downstream of the dam (Fig. 2), thus matching the geomorphological pattern described above.

In contrast to *várzea* habitats and most Andean rivers, the Uatumã River originates from the Guiana Shield, like most black water rivers in the middle portion of the Amazon basin (northern rivers) (Abad et al., 2013; IDESAM, 2009; Sioli, 1984). Black water rivers are stable and have slow geomorphologic and floristic dynamics, which can be associated to the presence of monodominant populations of ancient trees (Junk et al., 2015).

Since the damming of the Uatumã River by the Balbina hydroelectric plant, the annual predictable flood pulse has been modified (Assahira et al., 2017; Timpe and Kaplan, 2017). However, the only available water level monitoring station for the Uatumã River downstream of the dam is the Cachoeira Morena gauging station, operated by the Brazilian Geological Service/Brazilian National Water Agency (CPRM/ANA) (Cachoeira Morena Station - number 16100000). However, because this station sits on a terrace, near rapids, its data do not reflect the range of absolute river stage variation (see Fig. 2), and its overall measured stage amplitude (ca. 2 m) is much smaller than the observed amplitudes downriver (up to 9 m, field measurements). The lack of proper monitoring stations downriver makes it difficult to characterize the absolute magnitudes of changes in the water level regime post-damming.

Furthermore, as the hydrological regime is presently irregular, care must be taken to separate abnormal events caused by the dam from the effects of extreme climatic events. As a consequence of the strong El Niño event in1997/98 reducing rainfall in the Central Amazon region

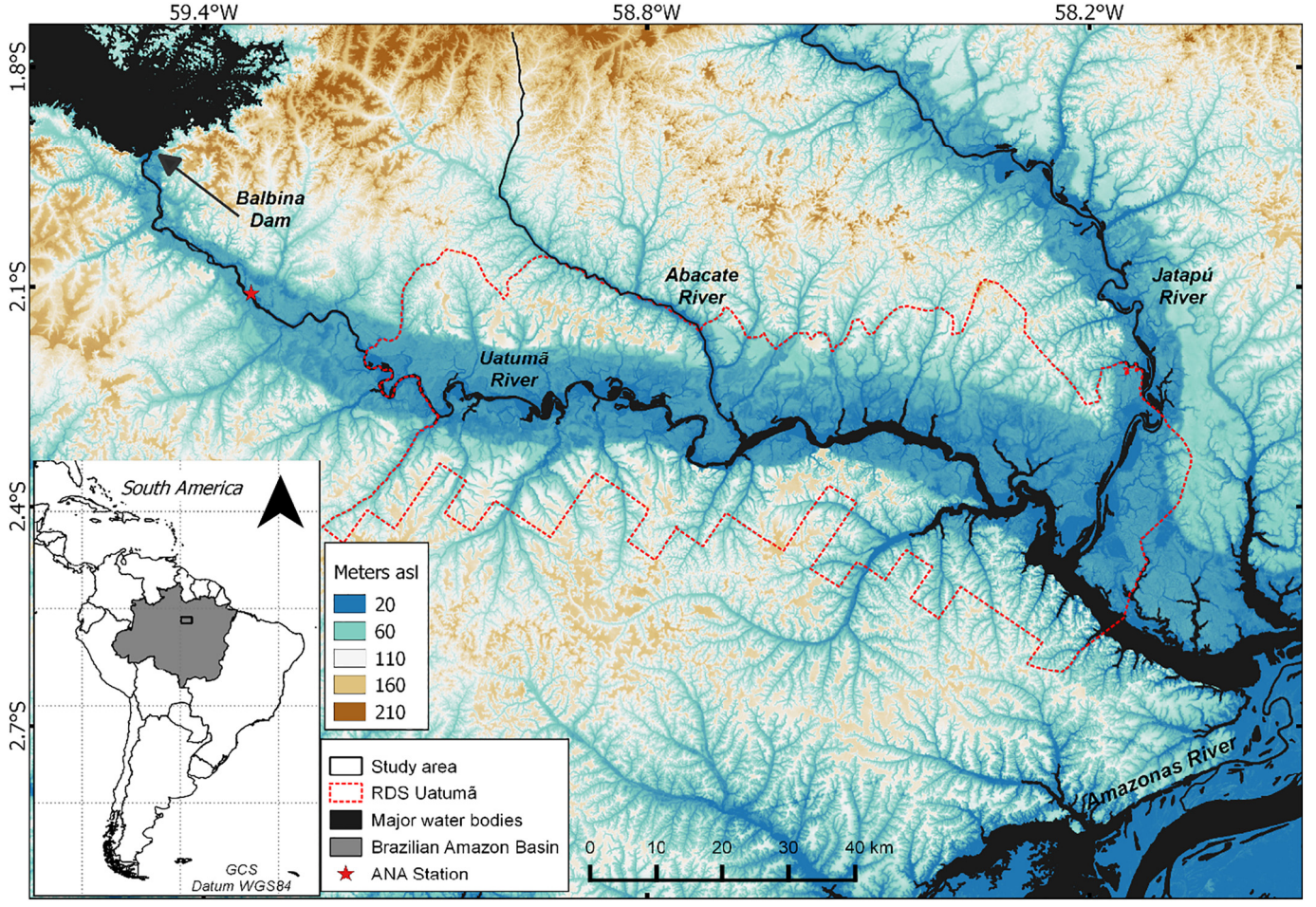

Fig. 1. Location of the study area in the Brazilian Amazon Basin, and detail of the study site, from the Balbina dam to the mouth of the Uatumã River. Background: Shuttle Radar Topography Mission digital elevation model showing the topographic variation with red outlines showing the areas mapped by remote sensing. (For interpretation of the references to colour in this figure legend, the reader is referred to the web version of this article.)

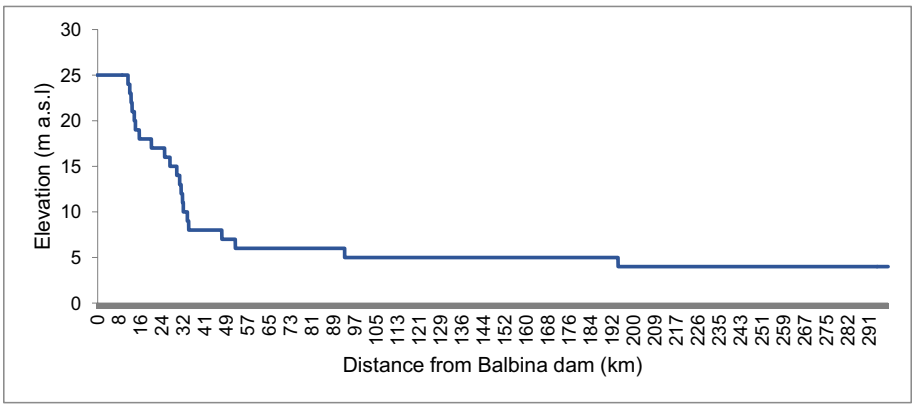

Fig. 2. Longitudinal elevation profile along the main Uatumã river channel (in February 2000) showing the steeper slope along the first 35 to 50 km downstream of the Balbina dam (SRTM data obtained from earthexplorer.usgs.gov).

(Foley et al., 2002; Marengo and Espinoza, 2016), all *igapós* were dry, followed by a 13-year period between 1999 and 2012, where all lower elevation *igapós* and some intermediate elevation *igapós* were completely flooded. In May 2000, water levels flooded all *igapós* for at least six days, reaching upland forests and riverine houses. During the severe El Niño event in 2015/16, water levels were so low that even the lowest areas including dead stands remained dry. This shows how unpredictable and irregular the flood pulse has become after starting hydropower operations, and the full consequences of such events remain unknown (Fig. 3).

2.2. Remote sensing data

We used L-band synthetic aperture radar (SAR) satellite images, as they have the ability to penetrate forest canopies and detect the flooding beneath, producing an increase in the returned signal (radar backscattering) known as "double-bounce" (Silva et al., 2015). Furthermore, L-band radar is insensitive to cloud cover and other atmospheric interferences like gases, smoke and illumination (Woodhouse, 2017). For our study, the detection of areas with high tree mortality is based on the even stronger SAR return signal caused by double-bounce between the free water surface and the standing dead trees, without the attenuation caused by volumetric scattering from canopies that is observed for live forest stands (Hess et al., 2002; Silva et al., 2008). In general, dead tree stands under flooded conditions have higher SAR returns than live flooded stands, which are still brighter than upland, non-flooded forests.

We acquired 56 SAR images from the Phased Array Type L-band Synthetic Aperture Radar (PALSAR) sensor, onboard the Advanced Land Observing Satellite-1 (ALOS-1), operated by the Japanese Aerospace Exploration Agency (JAXA), including 14 images for each of the following frame/path numbers: 7130/71, 7140/72, 7140/73, and 7140/74 (Table S1). The ALOS-1 mission operated between 2006 and 2011, carrying several sensors including PALSAR-1, a synthetic aperture radar operating at L-band with a wavelength of 23.5 cm. All images were acquired at the finest available resolution, in two polarization modes: Fine Beam Single (FBS) with HH polarization, and Fine Beam Dual (FBD) with HH and HV polarizations. The nominal spatial resolution after pre-processing was 25 m, and each scene covers a swath of approximately 70 km. All images were obtained from the Alaska Satellite Facility (vertex.daac.asf.alaska.edu/), at the Radiometric Terrain Corrected (RTC) processing level (ASF DAAC, 2015).

Since the ALOS/PALSAR mission did not perform regular observations of the Earth surface, unlike systems such as the well-known Landsat series, PALSAR images were selected from the historical record to maximize the range of flood amplitudes observed for our study site, based on the association between water stage heights observed in the Cachoeira Morena gauging station and image acquisition dates.

2.3. Image processing and classification

We adapted the approach previously used to classify Amazonian *várzea* environments, developed by Arnesen et al. (2013), Ferreira-Ferreira et al. (2014) and Silva et al. (2010). To adapt it for *igapó* forests, we had to consider the presence of a different floodplain structure, with

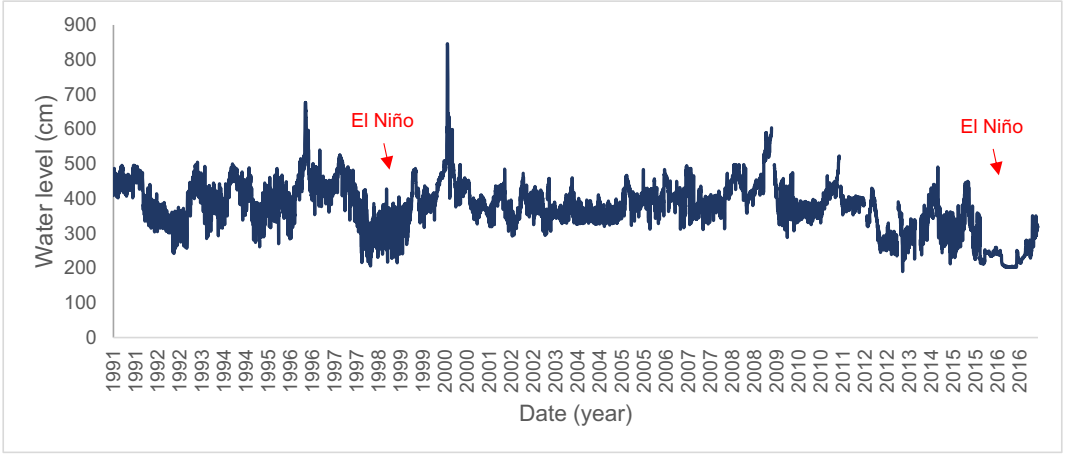

Fig. 3. The line shows the average water level during the post-dam period.

the occurrence of almost monospecific stands in lower topographies, capable of withstanding long periods of flooding (Junk et al., 2015).

Our approach is based on object-based image analysis (OBIA), where the image is first segmented into homogeneous groups of pixels (objects), which correspond to different elements of the landscape (Blaschke, 2010). Prior to segmentation, three seasonal descriptor images were calculated: (1) TBM - temporal backscattering mean, (2) TSD - temporal standard deviation of backscattering, and (3) BLW - backscattering at the lowest water level (Arnesen et al., 2013). These descriptors aid in the segregation of important landscape characteristics during segmentation, and they separate areas where there is less temporal variation from areas that change more in response to water level variation. The descriptors were converted to an 8-bit scale and filtered 3 times by a 3×3 window of a Gamma filter (Shi and Fung, 1994) to reduce speckle noise and increase the efficiency of the segmentation algorithm.

We used these three seasonal descriptors as inputs for the multiresolution segmentation algorithm from Benz et al. (2004), iteratively optimizing the algorithm parameters as scale = 70, shape = 0.1 and compactness = 0.5, to better represent homogeneous landscape units. After segmentation, we computed the mean and standard deviation of SAR backscatter for each object in each acquired image and for the three original untransformed and unfiltered seasonal descriptors (Fig. 4).

To train the classification algorithm, we used high-resolution images from Google Earth™ and Bing Maps™, loaded into the QGIS 2.18 software using the *OpenLayers Plugin*, combined with field GPS points and field knowledge, to select about 80 training samples for each of the five pre-defined land cover classes (Table 1).

We then used the sampled training objects as inputs to the Random Forests (RF) classification algorithm, implemented in the *Random Forest* package of the open source software R (Liaw and Wiener, 2002; R Core Team, 2017). This algorithm categorizes the segments using a "forest" of predictive trees, based on independent randomized samples (Breiman, 2001). The RF algorithm was applied following Ferreira-Ferreira et al. (2014), with the parameters *Number of Trees* and *Number of Variables Tried at Each Split* set as *ntree* = 15,000 and *mtry* = 20.

One important limitation of our method is that it relies on the increased double-bounce scattering caused by flooding to separate floodplain forests from upland forests. We are therefore unable to detect former floodplain areas that are no longer subject to regular flooding, and some of the areas classified as upland might represent additional lost *igapó* regions, assuming the loss of flooding will lead to changes in forest structure and composition over time.

2.4. Forecasting future forest mortality

In addition to mapping dead forest stands, we used remote sensing information to identify threatened areas that are still responding to the effects of altered hydrological conditions, and where mortality is likely to be ongoing. These areas do not yet show the high degrees of mortality that make dead stands distinguishable from living flooded forest stands in the radar images.

We measured local maximum water levels at 28 known field locations, represented by the high-water marks left on tree trunks during the last flood (before June 2017). We then assigned observed maximum water levels to their respective mapped objects, which we then grouped into four floodplain classes: "high *igapó*", "intermediate *igapó*", "low *igapó*" (high and low referencing terrain height, according to the Junk et al. (2015) classification) and "submerged", this last designation meaning areas that used to be low *igapó* but currently remain permanently flooded. From the images, we extracted backscattering coefficients from different dates and respective levels to represent each flood pulse phase: dry, low, medium and high water (Fig. 6).

We first analyzed the temporal radiometric behavior of each group of images corresponding to different periods of the hydrological

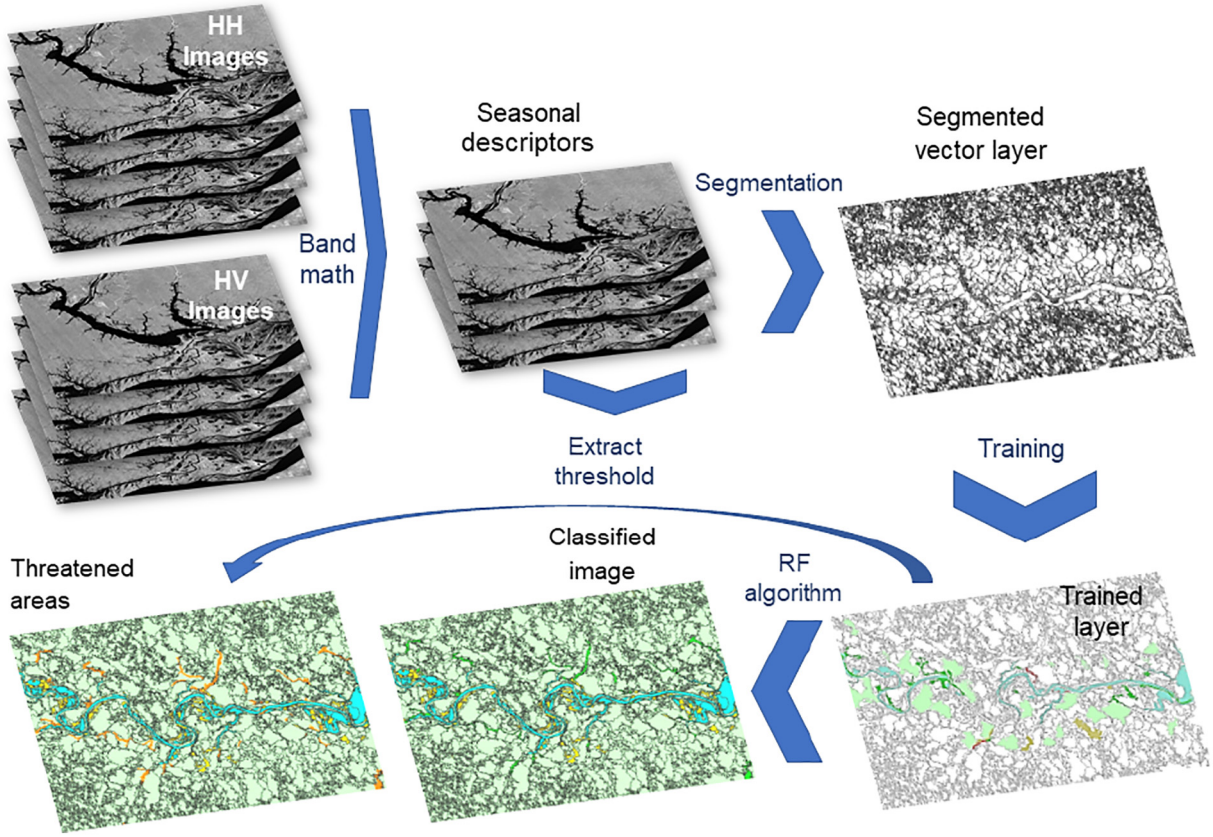

Fig. 4. Systematization of the stages of image processing, analysis and classification.

Fig. 5. Dead forest stands in the floodplains of the Uatumã River, below the blue line. Behind the dead stands, between the orange and blue lines, the igapó forest is observable, followed by upland (terra firme) forest above the orange line. (For interpretation of the references to colour in this figure legend, the reader is referred to the web version of this article.)

(flood-pulsing) regime for each floodplain class, to determine the best configuration to get good separability of classes based on the backscattered signal. Using an average image (n = 6) of the medium water level images (between 400 and 449 cm at Cachoeira Morena Station), we extracted the backscattering coefficients and applied a threshold to discriminate areas of "high", "intermediate", "low" and "submerged" *igapó*, this last class remaining flooded even during the average low water period. We defined a minimum mean flooding threshold of −4.48 dB to characterize areas that are now continuously flooded, and thereby likely undergoing mortality.

2.5. Validation

Classification accuracy was assessed using between 20 and 30 samples per vegetation class, based on high-resolution image interpretation and on observations made in the field in June of 2017, from a boat all along the focal area, using a GPS receiver. We applied the methods developed by Pontius and Millones (2011) and Pontius and Santacruz (2014) to verify the disagreement in class quantity and allocation, the latter subdivided into exchange and shift.

3. Results

Our classification using the random forests algorithm had an overall accuracy of 87.2% along the entire studied reach (Table S2). We mapped 9800 km^2 of flooded forest, 135 km^2 of non-forest areas and 13 km^2 of dead stands between the hydroelectric dam and the Uatumã river mouth (Fig. 7). Most flooded forest and water areas were located close to or within the confluence of the Uatumã River with the Amazon River. The water and upland classes were the most accurately classified, while the remaining three classes had some degree of confusion. Accuracy assessment showed the highest quantity disagreement errors as 12% for water and 6% for dead stands, respectively, while shift and exchange errors only occurred between flooded forest and non-forest classes, in small proportion (Fig. 8).

After mapping, we identified that, along the 300-km reach of the Uatumã River originally studied, massive mortality occurred mostly over a shorter reach, which we denominated the focal area (FA). The FA comprised an 80-km river reach beginning 43 km below the dam and included 90 km^2 of flooded forest and 50 km^2 of non-forest areas. Massive mortality within the FA covered about 11 km^2, 12% of the original flooded forest cover. The furthest mapped dead stand was observed at 123 km below the dam, and about 39 km before the confluence with Abacate River.

We mapped an additional 19 km^2 of threatened areas, defined as floodplain forests that are now almost continuously flooded, corresponding to an additional 18% of the original flooded forest cover within the focal area. Before the Balbina Dam was built, these areas were flooded for four to eight months, whereas now they are flooded for almost the entire year and are thus very likely to be undergoing slow mortality. If we include the mapped areas of dead stands and threatened areas within the focal area, c.a. 29% of the original *igapó* forest along the 80-km focal area of the Uatumã River has been strongly impacted by the Balbina Dam (Fig. 9).

Table 1
Land cover classes defined and used to train the Random Forests algorithm to identify igapó forests and tree mortality in the Uatumã River (Amazon, Brazil) using ALOS/PALSAR data.

Land cover class	Standing water presence	Canopy presence	Other characteristics
Dead stands	Yes	No	Mostly dense, dead standing trees under long periods of flooding (Fig. 5).
Flooded forests	Yes	Yes	Living trees at varying densities.
Non-forest	Occasionally	No	Grasslands, shrublands, woodlands, settlements (small villages and farms), sand banks and river beaches, campinas (herbaceous vegetation/shrubs in sandy soil).
Open water	Yes	No	Permanently open water surfaces
Upland	No	Yes	Any type of forest vegetation with a closed canopy (including some campinaranas) that never flood, this class was defined as mask, and not further quantified, although in some places this category included former floodplain no longer subject to inundation.

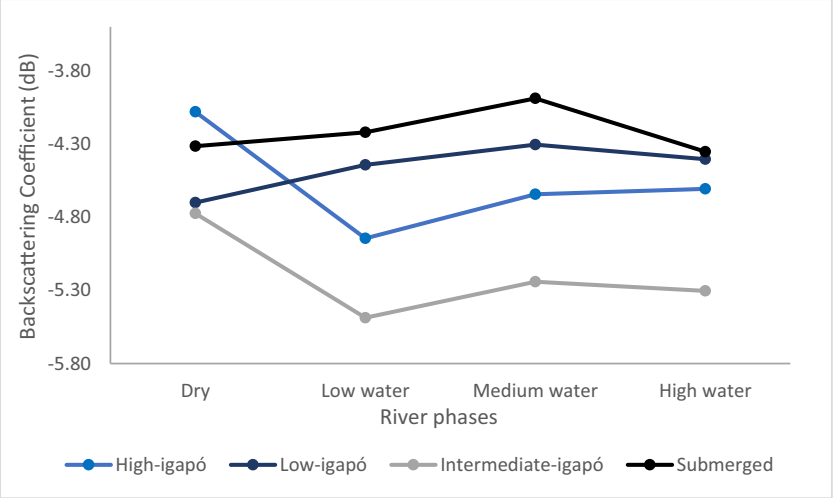

Fig. 6. L-band radar backscatter for different topographical levels of igapó forests at different periods of the flood-pulse regime.

4. Discussion

Our work shows that (1) there were significant losses of *igapó* forest downstream of the Balbina dam, caused by the changes in the flood pulse, and several areas are still undergoing mortality and may disappear in the near future; and (2) *igapó* forests are highly sensitive to hydrological disturbances linked to loss of flood pulse seasonality; (3) the downstream impacts caused by the dams are not trivial and need to be taken into account in environmental impact assessments and reports; (4) to preserve downstream forests, the maintenance of a

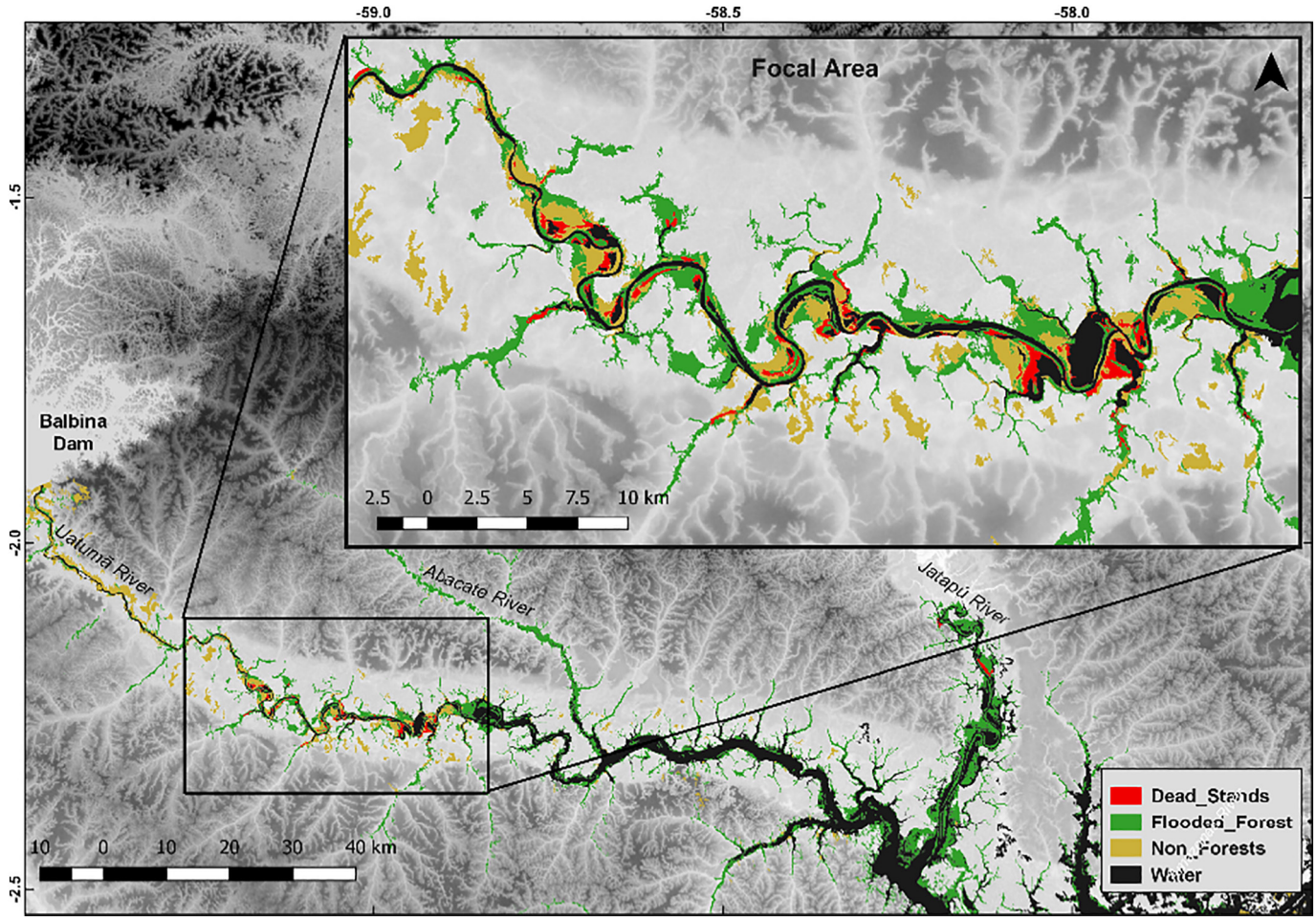

Fig. 7. Classification of the floodplains of the Uatumã River and its major tributaries (Abacate and Jatapú rivers) downstream of the Balbina dam. Dead forests occurred extensively along a stretch of about 80 km (focal area), between 43 and 123 km downstream of the Balbina hydroelectric power plant. Background: shaded relief derived from the SRTM digital elevation model.

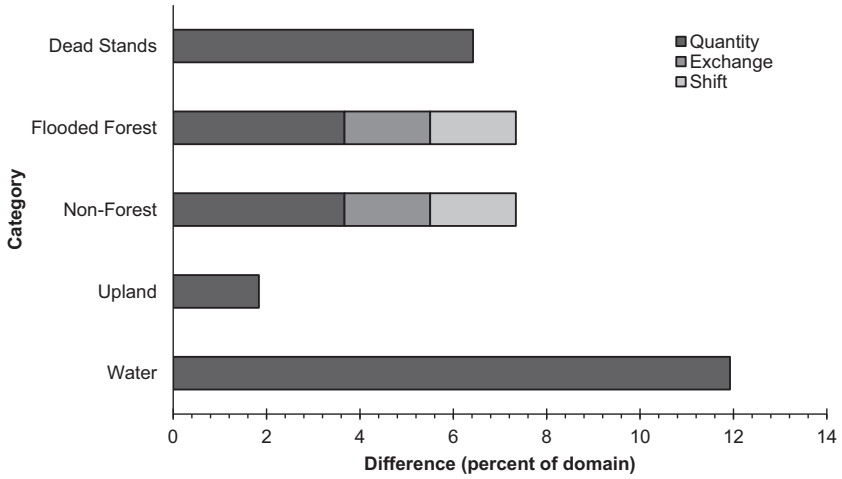

Fig. 8. Per-class disagreement between produced maps and ground-truth observations, following Pontius and Millones (2011) and Pontius and Santacruz (2014).

flood pulse that is the closest possible to the natural pulse in necessary as a mitigating action for Amazon hydroelectric projects, even if it results in reduced hydroelectric efficiency.

In the first 40 km immediately after the dam (and up to about 10 km downstream of the rapids of Cachoeira Morena), the Uatumã River follows a steep downslope along a narrow channel, where few flooded *igapós* can develop, explaining the absence of mapped floodplain forests and consequently dead stands. In addition, this reach is greatly altered by human settlements, with different land cover types and little natural vegetation left. The effects of flood pulse changes caused by Balbina are also less evident after 120 km downstream of the dam, where the abnormal discharge caused by damming seems to be attenuated by contributions from the two largest tributary rivers (Abacate and Jatapú Rivers) and, at some point, by the Amazon River backwater effect (Meade et al., 1991).

Massive mortality occurred along regions where specific hydrogeomorphological conditions favored the formation of large floodplain forests controlled exclusively by the Uatumã River flood

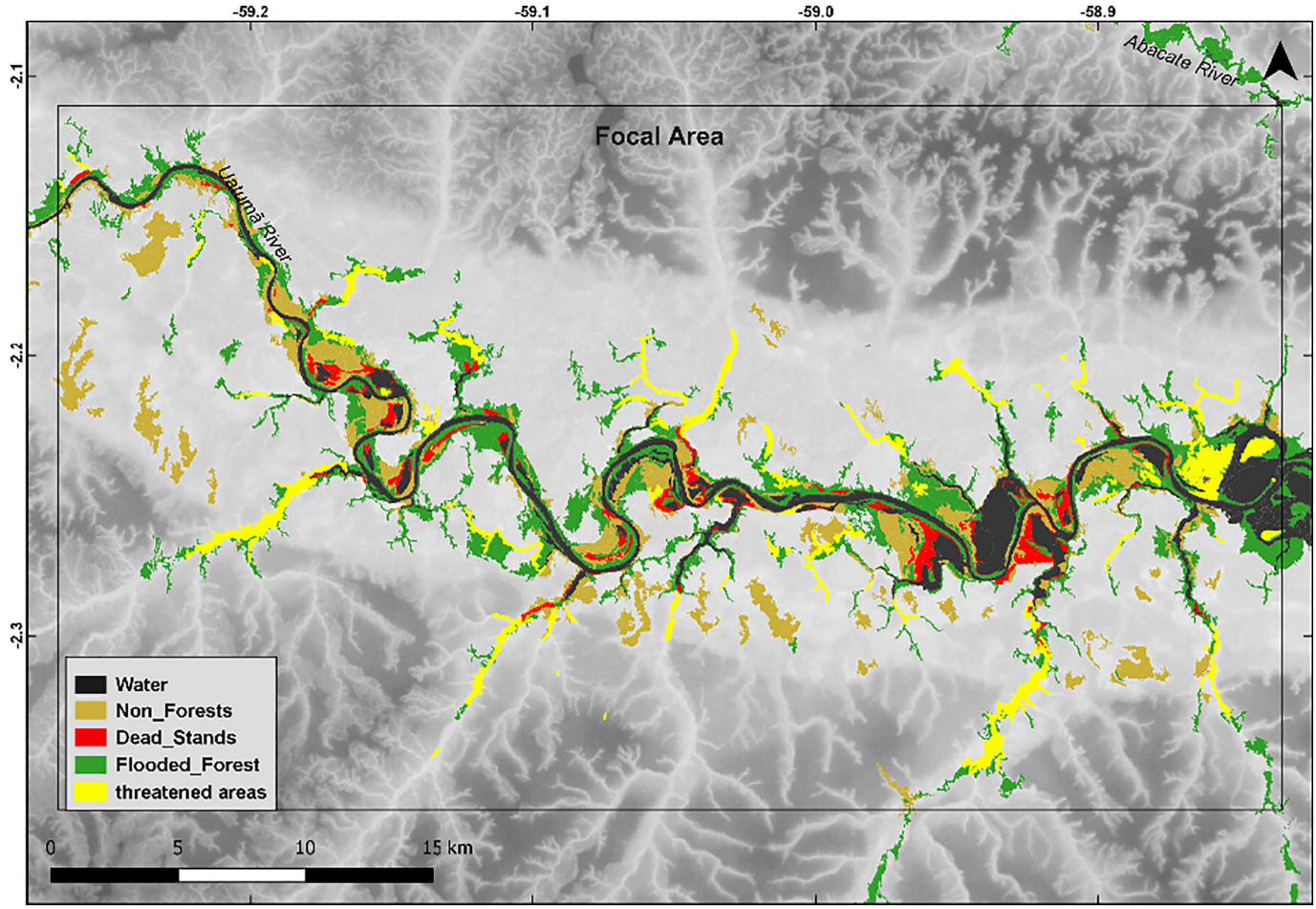

Fig. 9. Map shows potentially threatened areas adjacent to dead stands. These areas can spend entire years flooded, depending on the management of river flow by the hydropower facility.

pulse, corresponding to the reach starting 43 km after the dam and ending before the Abacate River mouth. Also, almost all dead stands were located on the insides of channel meanders, further emphasizing the connection between channel morphology and ecological impacts. Our findings corroborate Assahira et al. (2017), who made field observations of dead trees for about 100 km below the Balbina Dam.

It is important to note that our method only detects dead forest stands and potential ongoing mortality areas when they are located below current maximum flooding levels, and thus still exhibit some double-bounce response in the image series. Despite comprising a third of all flooded forest areas, these classes may not represent the entirety of lost *igapó* forests downstream; there are several past floodplain areas which are now topographically above the current maximum flooding heights and are no longer annually flooded, nor do they remain flooded for a predictable time. This change will very likely lead to profound changes in species composition, community structure and ecosystem processes over time, as the forest transitions to upland forest structure and dynamics, and thus represents a yet to be quantified additional amount of *igapó* forest loss (Assahira et al., 2017; Lobo et al., 2019).

High flood tolerance is also not a protection from the effects of flood pulse changes. In black-water *igapó* floodplains, a few tree species have the necessary adaptations to tolerate very long periods of flooding (up to 300 days per year), forming monodominant or even monospecific stands. One of the most frequent tree species in this category is *Eschweilera tenuifolia* (O. Berg) Miers, locally known as *Macacarecuia* (Junk et al., 2015; Mori and Prance, 1990). Despite being highly flood-tolerant, we observed several populations of this species suffering massive mortality within the studied area. Massive mortality was also observed for populations of the less frequent species *Macrolobium acaciifolium* within the same or similar areas, at slightly higher elevations of the Uatumã floodplains (Assahira et al., 2017).

Furthermore, a compound effect of the mortality of established adult plants is that changes in the hydrological cycle may create a barrier to seed dispersal and germination, which are generally synchronized with the flood pulse (Oliveira-Wittmann et al., 2010). Oxygen limitation in soil due to uninterrupted flooding can also lead to high mortality of potentially regenerating soil seeds and young saplings (Yang and Li, 2013), as establishment and recruitment occurs when the soil is exposed by the receding water levels (Parolin et al., 2010).

In the Central Amazonian floodplains, multiannual extreme wet and dry periods can also have dramatic effects, such as the 1971–75 period when a large-scale dieback of shrubs and trees colonizing the lowest elevations of *várzeas* and *igapós* was observed (Piedade et al., 2012). Junk (1989) related this phenomenon to a multiannual period of abnormally high minimum water levels caused by several La Niña events (Marengo, 2009; Schöngart and Junk, 2007). During strong El Niño events, the black-water *igapós* along the Negro River and other blackwater rivers are also especially vulnerable to wildfires (Flores et al., 2014; Resende et al., 2014; Sombroek, 2001), as the El Niño-induced rainfall anomalies coincide with the low-water periods of these rivers, with strong implications for plant-water availability (Schöngart et al., 2017). Large-scale fires were reported for the El Niño-induced droughts in 1925/26 (Williams et al., 2005), 1997/98 (Flores et al., 2014; Nelson, 2001) and 2015/16 (Aragão et al., 2018). These climatic vulnerabilities are expected to become more frequent in the future and may further compound the effects of river damming on floodplain forests.

Igapó ecosystems are more susceptible to wildfire than uplands (*terra firme*) or *várzeas*, due to the scarcity of nutrients and the long-term flooding that leads to an accumulation of root mats and litter on the surface, and to a drier microclimate when they are not flooded (de Almeida et al., 2016; Dos Santos and Nelson, 2013; Flores et al., 2014; Resende et al., 2014). The large amounts of dead biomass resulting from mass mortality induced by hydroelectric damming, associated with the drier microclimate in these forests, could make these ecosystems even more susceptible to wildfires (de Almeida et al., 2016; Cochrane et al., 1999; Flores et al., 2017; Kauffman et al., 1988; Resende et al., 2014). Therefore, rising temperatures and increasing drought frequency and intensity (Gloor et al., 2013, 2015; Marengo and Espinoza, 2016) combined with land-use changes associated with deforestation and fire (Aragão et al., 2018; Nobre et al., 2016), as well as the implementation of construction of additional hydroelectric dams (Forsberg et al., 2017; Lees et al., 2016), may severely impact the *igapó* ecosystems in the future.

Massive mortality will also have several impacts on the entire ecosystem, such as niche and diversity losses, changes in community structure, facilitation of pests and diseases, and changes in biogeochemical cycles (Cherubini et al., 2002; Franklin et al., 1987). Even edge-related tree mortality on upland forests (Mesquita et al., 1999) can became a problem if the "buffer" provided by *igapó* forests is broken and adjacent upland forests are exposed. For the lowest-lying *igapós* of the Uatumã River, the carbon stock of aboveground biomass has been estimated at 118 ± 12.8 Mg C ha^{-1} (Neves, 2018). Considering the area of dead forests calculated in the present study as a conservative estimate (10.9 km^2), we can estimate a biomass loss of $129 \pm 14 \times 10^9$ g C. However, as the total mortality process is expected to affect 30 km^2 of forests (29% of the original *igapó*), biomass loss may reach $354 \pm 38 \times 10^9$ g. This would further worsen Balbina's greenhouse gas emissions budget, estimated at 2.5×10^{12} g C (CO_2 equivalent emissions) due to increased methane (CH_4) emissions from the reservoir area (Fearnside, 1995; Kemenes et al., 2011).

In summary, our study confirms that threats to floodplains downstream of hydropower enterprises are evident, and the environmental effects of existing and proposed hydroelectric dams need to be better understood in Amazonia and other wetlands at risk (Junk et al., 2014; Kingsford, 2000; Zahar et al., 2008; Ziegler et al., 2013). Furthermore, this information must be considered when licensing and quantifying the environmental impacts of these enterprises. The legal instrument that assists the Brazilian government in making decisions about large infrastructure projects is the Environmental Impact Assessment (EIA; *Estudo de Impacto Ambiental* in Portuguese), and its accompanying Environmental Impacts Report (RIMA, in Portuguese), which must characterize the environmental conditions of an area prior to the approval of a proposed project, and must indicate all potential impacts, as well as proposing mitigating measures when appropriate (Brasil, 1986). However, the Brazilian Amazon EIA/RIMAs are often disregarded during decision making (Cochrane et al., 2017; Ritter et al., 2017). Our suggestion is to improve their diagnostic and predictive power, complementing the impact reports with surveys downstream of affected areas, as well as dynamic projective analyses of changes and predicted flood-pulse pattern after damming.

Although we could map the most fragile areas, it is still difficult to predict the exact duration and extent of the ongoing tree mortality process due to the alteration of the flood pulse. It is likely, however, that it will last for decades to come (Assahira et al., 2017) and that climate change and land-use interactions will probably intensify the deleterious effects caused by dams in the Amazon (Nobre et al., 2016). Fearnside (2016) raised the following question: "Tropical dams: to build or not to build?" Our study adds to previous evidence that the negative environmental and social effects of tropical hydropower dams are enormous, and that these effects can reach distant areas, yet they can be overlooked by scientific studies and not considered in EIA/RIMAs. This framework needs to change, and the available science must be considered to support decision-making.

Acknowledgments

We thank the two anonymous reviewers and Megan F. King who directly contributed to this paper, the National Institute for Amazon Research (INPA), the PELD/MAUA group, and the Ecosystem Dynamics Observatory at the Universidade Estadual Paulista "Júlio de Mesquita Filho" (UNESP Rio Claro) for support and data provision. We also thank

the RDS Uatumã and ATTO project for the infrastructure and work support, and the Brazilian Council for Scientific Research (CNPq) for financing the project and the PhD fellowship of AF Resende (MCTI/CNPq/FNDCT n° 68/2013 - Large-Scale Biosphere-Atmosphere Program in the Amazon - LBA), PELD-MAUA project (403792/2012-6 - MCTI/CNPq/FAPs N° 34/2012 and 441590/2016-0-CNPq/CAPES/FAPS/BC-Fundo Newton). We also thank the Alaska Satellite Facility for providing the ALOS/PALSAR images. This work was conducted within the framework of the Kyoto & Carbon Initiative of the Japanese Aerospace Agency (JAXA). AS Streher acknowledges PhD fellowship #2015/17534-3, São Paulo Research Foundation, and TSF Silva acknowledges CNPq productivity grant #310144/2015-9.

Appendix A. Supplementary data

Supplementary data to this article can be found online at https://doi.org/10.1016/j.scitotenv.2018.12.208.

References

Abad, J.D., Vizcarra, J., Paredes, J., Montoro, H., Frias, C., Holguin, C., 2013. Morphodynamics of the upper Peruvian Amazonian rivers, implications into fluvial transportation. Int. Conf. IDS2013 - Amaz., pp. 1–10

Adeney, J.M., Christensen, N.L., Vicentini, A., Cohn-Haft, M., 2016. White-sand ecosystems in Amazonia. Biotropica 48, 7–23. https://doi.org/10.1111/btp.12293.

Anderson, E.P., Jenkins, C.N., Heilpern, S., Maldonado-ocampo, J.A., Carvajal-vallejos, F.M., Encalada, A.C., Rivadeneira, J.F., 2018. Fragmentation of Andes-to-Amazon connectivity by hydropower dams. Sci. Adv. 1–8. https://doi.org/10.1126/sciadv.aao1642.

Andreae, M.O., Acevedo, O.C., Araùjo, A., Artaxo, P., Barbosa, C.G.G., Barbosa, H.M.J., Brito, J., Carbone, S., Chi, X., Cintra, B.B.L., Da Silva, N.F., Dias, N.L., Dias-Júnior, C.Q., Ditas, F., Ditz, R., Godoi, A.F.L., Godoi, R.H.M., Heimann, M., Hoffmann, T., Kesselmeier, J., Könemann, T., Krüger, M.L., Lavric, J.V., Manzi, A.O., Lopes, A.P., Martins, D.L., Mikhailov, E.F., Moran-Zuloaga, D., Nelson, B.W., Nölscher, A.C., Santos Nogueira, D., Piedade, M.T.F., Pöhlker, C., Pöschl, U., Quesada, C.A., Rizzo, L.V., Ro, C.U., Ruckteschler, N., Sá, L.D.A., De Oliveira Sá, M., Sales, C.B., Dos Santos, R.M.N., Saturno, J., Schöngart, J., Sörgel, M., De Souza, C.M., De Souza, R.A.F., Su, H., Targhetta, N., Tóta, J., Trebs, I., Trumbore, S., Van Eijck, A., Walter, D., Wang, Z., Weber, B., Williams, J., Winderlich, J., Wittmann, F., Wolff, S., Yáñez-Serrano, A.M., 2015. The Amazon Tall Tower Observatory (ATTO): overview of pilot measurements on ecosystem ecology, meteorology, trace gases, and aerosols. Atmos. Chem. Phys. 15, 10723–10776. https://doi.org/10.5194/acp-15-10723-2015.

Aragão, L.E.O.C., Anderson, L.O., Fonseca, M.G., Rosan, T.M., Vedovato, L.B., Wagner, F.H., Silva, C.V.J., Silva Junior, C.H.L., Arai, E., Aguiar, A.P., Barlow, J., Berenguer, E., Deeter, M.N., Domingues, L.G., Gatti, L., Gloor, M., Malhi, Y., Marengo, J.A., Miller, J.B., Phillips, O.L., Saatchi, S., 2018. 21st century drought-related fires counteract the decline of Amazon deforestation carbon emissions. Nat. Commun. 9, 1–12. https://doi.org/10.1038/s41467-017-02771-y.

Arnesen, A.S., Silva, T.S.F., Hess, L.L., Novo, E.M.L.M., Rudorff, C.M., Chapman, B.D., McDonald, K.C., 2013. Monitoring flood extent in the lower Amazon River floodplain using ALOS/PALSAR ScanSAR images. Remote Sens. Environ. 130, 51–61. https://doi.org/10.1016/j.rse.2012.10.035.

ASF DAAC, 2015. ASF DAAC. PALSAR_Radiometric_Terrain_Corrected_high_res [WWW Document]. Incl. Mater. © JAXA/METI 2007. https://doi.org/10.5067/Z97HFCNKR6VA.

Assahira, C., de Resende, A.F., Trumbore, S.E., Wittmann, F., Cintra, B.B.L., Batista, E.S., 2017. Tree mortality of a flood-adapted species in response of hydrographic changes caused by an Amazonian river dam. For. Ecol. Manag. 396, 113–123. https://doi.org/10.1016/j.foreco.2017.04.016.

Benchimol, M., Peres, C.A., 2015. Edge-mediated compositional and functional decay of tree assemblages in Amazonian forest islands after 26 years of isolation. J. Ecol. 103, 408–420. https://doi.org/10.1111/1365-2745.12371.

Benz, U.C., Hofmann, P., Willhauck, G., Lingenfelder, I., Heynen, M., 2004. Multi-resolution, object-oriented fuzzy analysis of remote sensing data for GIS-ready information. ISPRS J. Photogramm. Remote Sens. 58, 239–258. https://doi.org/10.1016/j.isprsjprs.2003.10.002.

Blaschke, T., 2010. Object based image analysis for remote sensing. ISPRS J. Photogramm. Remote Sens. 65, 2–16. https://doi.org/10.1016/j.isprsjprs.2009.06.004.

Brasil, 1986. Resolução CONAMA nº 01, de 23 de Janeiro de 1986. CONAMA - Cons. Nacinal o Meio Ambient https://doi.org/10.1017/CBO9781107415324.004.

Breiman, L., 2001. Random forests. Mach. Learn. 45, 5–32. https://doi.org/10.1023/A:1010933404324.

Castello, L., Macedo, M.N., 2016. Large-scale degradation of Amazonian freshwater ecosystems. Glob. Chang. Biol. 22, 990–1007. https://doi.org/10.1111/gcb.13173.

Castello, L., Mcgrath, D.G., Hess, L.L., Coe, M.T., Lefebvre, P.A., Petry, P., Macedo, M.N., Renó, V.F., Arantes, C.C., Ren, V.F., Arantes, C.C., 2013. The vulnerability of Amazon freshwater ecosystems. Conserv. Lett. 6, 217–229. https://doi.org/10.1111/conl.12008.

Cherubini, P., Fontana, G., Rigling, D., Dobbertin, M., Brang, P., Innes, J.L., 2002. Tree-life history prior to death: two fungal root pathogens affect tree-ring growth differently. J. Ecol. 90, 839–850.

Cochrane, M.A., Alencar, A., Schulze Jr., M.D., Souza, C.M., Nepstad, D.C., Lefebvre, P., Davidson, E.A., 1999. Positive feedbacks in the fire dynamic of closed canopy tropical forests. Science 284, 1832–1835.

Cochrane, S.M.V., Matricardi, E.A.T., Numata, I., Lefebvre, P.A., 2017. Landsat-based analysis of mega dam flooding impacts in the Amazon compared to associated environmental impact assessments: Upper Madeira River example 2006–2015. Remote Sens. Appl. Soc. Environ. 7, 1–8. https://doi.org/10.1016/j.rsase.2017.04.005.

de Almeida, D.R.A., Nelson, B.W., Schietti, J., Gorgens, E.B., Resende, A.F., Stark, S.C., Valbuena, R., 2016. Contrasting fire damage and fire susceptibility between seasonally flooded forest and upland forest in the Central Amazon using portable profiling LiDAR. Remote Sens. Environ. 184, 153–160. https://doi.org/10.1016/j.rse.2016.06.017.

De Simone, O., Junk, W.J., Schmidt, W., 2003. Central Amazon floodplain forests: root adaptations to prolonged flooding. Russ. J. Plant Physiol. 50, 848–855. https://doi.org/10.1023/B:RUPP.0000003285.70058.4c.

Dos Santos, A.R., Nelson, B.W., 2013. Leaf decomposition and fine fuels in floodplain forests of the Rio Negro in the Brazilian Amazon. J. Trop. Ecol. 29, 455–458. https://doi.org/10.1017/S0266467413000485.

Fearnside, P.M., 1989. Brazil's Balbina Dam: environment versus the legacy of the pharaohs in Amazonia. Environ. Manag. 13, 401–423. https://doi.org/10.1007/BF01867675.

Fearnside, P.M., 1995. Hydroelectric dams in the Brazilian Amazon as sources of 'greenhouse' gases. Environ. Conserv. 22, 7–19.

Fearnside, P.M., 2014. Impacts of Brazil's Madeira River Dams: unlearned lessons for hydroelectric development in Amazonia. Environ. Sci. Pol. 38, 164–172. https://doi.org/10.1016/j.envsci.2013.11.004.

Fearnside, P.M., 2016. Tropical dams: to build or not to build? Science https://doi.org/10.1126/science.351.6272.456-b (80-.).

Ferreira, L., Parolin, P., 2011. Effects of flooding duration on plant demography in a blackwater floodplain forest in central Amazonia. Pesqui Bot 323–332.

Ferreira-Ferreira, J., Silva, T.S.F., Streher, A.S., Affonso, A.G., De Almeida Furtado, L.F., Forsberg, B.R., Valsecchi, J., Queiroz, H.L., De Moraes Novo, E.M.L., 2014. Combining ALOS/PALSAR derived vegetation structure and inundation patterns to characterize major vegetation types in the Mamirauá Sustainable Development Reserve, Central Amazon floodplain, Brazil. Wetl. Ecol. Manag. 23, 41–59. https://doi.org/10.1007/s11273-014-9359-1.

Finer, M., Jenkins, C.N., 2012. Proliferation of hydroelectric dams in the Andean Amazon and implications for Andes-Amazon connectivity. PLoS One 7, 1–9. https://doi.org/10.1371/journal.pone.0035126.

Flores, B.M., Piedade, M.T.F., Nelson, B.W., 2014. Fire disturbance in Amazonian blackwater floodplain forests. Plant Ecolog. Divers. 7, 319–327. https://doi.org/10.1080/17550874.2012.716086.

Flores, B.M., Holmgren, M., Xu, C., van Nes, E.H., Jakovac, C.C., Mesquita, R.C.G., Scheffer, M., 2017. Floodplains as an Achilles' heel of Amazonian forest resilience. Proc. Natl. Acad. Sci. 114, 4442–4446. https://doi.org/10.1073/pnas.1617988114.

Foley, J.A., Botta, A., Coe, M.T., Costa, M.H., 2002. El Niño-Southern oscillation and the climate, ecosystems and rivers of Amazonia. Glob. Biogeochem. Cycles 16, 79-1–79-20. https://doi.org/10.1029/2002GB001872.

Foote, a.L., Pandey, S., Krogman, N.T., 1996. Processes of wetland loss in India. Environ. Conserv. 23, 45. https://doi.org/10.1017/S0376892900038248.

Forsberg, B.R., Melack, J.M., Dunne, T., Barthem, R.B., Goulding, M., Paiva, R.C.D., Sorribas, M.V., Silva, U.L., Weisser, S., 2017. The potential impact of new Andean dams on Amazon fluvial ecosystems. PLoS One https://doi.org/10.1371/journal.pone.0182254.

Franklin, J.F., Shugart, H.H., Harmon, M.E., 1987. Tree death as an ecological process. Bioscience 37, 550–556. https://doi.org/10.2307/1310665.

Gloor, M., Brienen, R.J.W., Galbraith, D., Feldpausch, T.R., Schöngart, J., Guyot, J.L., Espinoza, J.C., Lloyd, J., Phillips, O.L., 2013. Intensification of the Amazon hydrological cycle over the last two decades. Geophys. Res. Lett. 40, 1729–1733. https://doi.org/10.1002/grl.50377.

Gloor, M., Barichivich, J., Ziv, G., Brienen, R., Schöngart, J., Peylin, P., 2015. Recent Amazon Climate as Background for Possible Ongoing Special Section. https://doi.org/10.1002/2014GB005080.Received.

Hess, L.L., Novo, E.M.L.M., Slaymaker, D.M., Holt, J., Steffen, C., Valeriano, D.M., Mertes, L.A.K., Krug, T., Melack, J.M., Gastil, M., Holmes, C., Hayward, C., 2002. Geocoded digital videography for validation of land cover mapping in the Amazon basin. Int. J. Remote Sens. 23, 1527–1556. https://doi.org/10.1080/01431160110092687.

IDESAM, I. de C. e D.S. do A, 2009. Série Técnica Planos de Gestão Reserva de Desenvolvimento Sustentável do Uatumã Volumes 1 e 2 1 and 2, 150.

International Rivers, F.P., ECOA, 2017. Dams in Amazonia. [WWW Document]. Dams Amaz. URL. http://www.dams-info.org/en#, Accessed date: 4 September 2018.

Junk, W.J., 1989. Flood tolerance and tree distribution in central Amazonian floodplains. Tropical Forests: Botanical Dynamics, Speciation and Diversity https://doi.org/10.1016/B978-0-12-353550-4.50012-5.

Junk, W.J., Mello, J.A.S.N., 1990. Impactos ecológicos das represas hidrelétricas na bacia amazônica brasileira. Estud. Avançados 4, 126–143. https://doi.org/10.1590/S0103-40141990000100010.

Junk, W.J., Bayley, P.B., Sparks, R.E., 1989. The flood pulse concept in river-floodplain systems. Can. Spec. Publ. Fish. Aquat. Sci. 106, 110–127. https://doi.org/10.1371/journal.pone.0028909.

Junk, W.J., Piedade, M.T.F., Schöngart, J., Cohn-Haft, M., Adeney, J.M., Wittmann, F., 2011. A classification of major naturally-occurring Amazonian lowland wetlands. Wetlands 31, 623–640. https://doi.org/10.1007/s13157-011-0190-7.

Junk, W.J., Piedade, M.T.F., Lourival, R., Wittmann, F., Kandus, P., Lacerda, L.D., Bozelli, R.L., Esteves, F.A., Nunes da Cunha, C., Maltchik, L., Schöngart, J., Schaeffer-Novelli, Y., Agostinho, A.A., 2014. Brazilian wetlands: their definition, delineation, and

classification for research, sustainable management, and protection. Aquat. Conserv. Mar. Freshwat. Ecosyst. 24, 5–22. https://doi.org/10.1002/aqc.2386.
Junk, W.J., Wittmann, F., Schöngart, J., Piedade, M.T.F., 2015. A classification of the major habitats of Amazonian black-water river floodplains and a comparison with their white-water counterparts. Wetl. Ecol. Manag. 23, 677–693. https://doi.org/10.1007/s11273-015-9412-8.
Kahn, J.R., Freitas, C.E., Petrere, M., 2014. False shades of green: the case of Brazilian Amazonian hydropower. Energies 7, 6063–6082. https://doi.org/10.3390/en7096063.
Kauffman, J.B., Uhl, C., Cummings, D.L., 1988. Fire in the Venezuelan Amazon 1: fuel biomass and fire chemistry in the evergreen rainforest of Venezuela. Oikos 53, 167. https://doi.org/10.2307/3566059.
Kemenes, A., Forsberg, B.R., Melack, J.M., 2007. Methane release below a tropical hydroelectric dam. Geophys. Res. Lett. 34, 1–5. https://doi.org/10.1029/2007GL029479.
Kemenes, A., Forsberg, B.R., Melack, J.M., 2011. CO2 emissions from a tropical hydroelectric reservoir (Balbina, Brazil). J. Geophys. Res. Biogeosci. 116. https://doi.org/10.1029/2010JG001465.
Kingsford, R.T., 2000. Ecological impacts of dams, water diversions and river management on floodplain wetlands in Australia. Austral Ecol. 25, 109–127. https://doi.org/10.1046/j.1442-9993.2000.01036.x.
Latrubesse, E.M., Arima, E.Y., Dunne, T., Park, E., Baker, V.R., D'Horta, F.M., Wight, C., Wittmann, F., Zuanon, J., Baker, P.A., Ribas, C.C., Norgaard, R.B., Filizola, N., Ansar, A., Flyvbjerg, B., Stevaux, J.C., 2017. Damming the rivers of the Amazon basin. Nature 546, 363–369. https://doi.org/10.1038/nature22333.
Lees, A.C., Peres, C.A., Fearnside, P.M., Schneider, M., Zuanon, J.A.S., 2016. Hydropower and the future of Amazonian biodiversity. Biodivers. Conserv. 25, 451–466. https://doi.org/10.1007/s10531-016-1072-3.
Lewis, W.M., Hamilton, S.K., Lasi, M.a., Rodríguez, M., Saunders, J.F., 2000. Ecological determinism on the Orinoco floodplain. Bioscience 50, 681. https://doi.org/10.1641/0006-3568(2000)050[0681:EDOTOF]2.0.CO;2.
Liaw, A., Wiener, M., 2002. Classification and regression by randomForest. R News 2, 18–22. https://doi.org/10.1177/154405910408300516.
Ligon, F.K., Dietrich, W.E., Trush, W.J., 1995. Downstream ecological effects of dams. Bioscience 45, 183–192. https://doi.org/10.2307/1312557.
Lobo, G.S., Wittmann, F., Piedade, M.T.F., 2019. Response of black-water floodplain (igapó) forests to flood pulse regulation in a dammed Amazonian river. For. Ecol. Manag. 434, 110–118.
Manyari, W.V., de Carvalho, O.A., 2007. Environmental considerations in energy planning for the Amazon region: downstream effects of dams. Energy Policy 35, 6526–6534. https://doi.org/10.1016/j.enpol.2007.07.031.
Marengo, J.A., 2009. Long-term trends and cycles in the hydrometeorology of the Amazon basin since the late 1920s. Hydrol. Process. 23, 3236–3244.
Marengo, J.A., Espinoza, J.C., 2016. Extreme seasonal droughts and floods in Amazonia: causes, trends and impacts. Int. J. Climatol. 36, 1033–1050. https://doi.org/10.1002/joc.4420.
Meade, R.H., Rayol, J.M., Conceicão, S.C., Natividade, J.R.G., 1991. Backwater effects in the Amazon River basin of Brazil. Environ. Geol. Water Sci. https://doi.org/10.1007/BF01704664.
Melack, J.M., Hess, L.L., 2010. Remote sensing of the distribution and extent of wetlands in the Amazon basin. Amazonian Floodplain Forests. Springer, pp. 43–59.
Mesquita, R.C.G., Delamônica, P., Laurance, W.F., 1999. Effect of surrounding vegetation on edge-related tree mortality in Amazonian forest fragments. Biol. Conserv. 91, 129–134. https://doi.org/10.1016/S0006-3207(99)00086-5.
Mori, S.A., Prance, G.T., 1990. Flora Neotropica Monograph 21 (II) Lecythidaceae - Part II. The Zygomorphic-Flowered New World Genera (*Couroupita*, *Corythophora*, *Bertholletia*, *Couratari*, *Eschweilera* & *Lecythis*), Source: Flora Neotropica Aiphanes (Palmae). https://doi.org/10.2307/2805360.
Mumba, M., Thompson, J.R., 2005. Hydrological and ecological impacts of dams on the Kafue Flats floodplain system, southern Zambia. Phys. Chem. Earth 30, 442–447. https://doi.org/10.1016/j.pce.2005.06.009.
Nelson, B.W., 2001. Fogo em florestas da Amazônia Central em 1997. An. X SBSR 1675–82.
Neves, J.R.D., 2018. Mudanças na fitofisionomia e estoque e produção de biomassa pelas alterações no ciclo hidrológico em florestas alagáveis de igapó na Amazônia Central. Instituto Nacional de Pesquisas da Amazônia.
Nilsson, Christer, 2000. Alterations of riparian ecosystems caused by river regulation. AIBS Bull. 50, 783–792. https://doi.org/10.1641/0006-3568(2000)050[0783:aorecb]2.0.co;2.
Nobre, C.A., Sampaio, G., Borma, L.S., Castilla-Rubio, J.C., Silva, J.S., Cardoso, M., 2016. Land-use and climate change risks in the Amazon and the need of a novel sustainable development paradigm. Proc. Natl. Acad. Sci. 113, 10759–10768. https://doi.org/10.1073/pnas.1605516113.
Oliveira-Wittmann, A., Lopes, A., Conserva, A.D.S., Wittmann, F., Piedade, M.T.F., 2010. Seed germination and seedling establishment of Amazonian floodplain trees. Amazonian Floodplain Forests. Springer, pp. 259–280.
Parolin, P., De Simone, O., Haase, K., Waldhoff, D., Rottenberger, S., Kuhn, U., Kesselmeier, J., Kleiss, B., Schmidt, W., Piedade, M.T.F., Junk, W.J., 2004. Central Amazonian floodplain forests: tree adaptations in a pulsing system. Bot. Rev. 70, 357–380. https://doi.org/10.1663/0006-8101(2004)070[0357:CAFFTA]2.0.CO;2.
Parolin, P., Waldhoff, D., Piedade, M.T.F., 2010. Fruit and seed chemistry, biomass and dispersal. Amazonian Floodplain Forests. Springer, pp. 243–258.
Piedade, M.T.F., Wittmann, F., Parolin, P., Junk, W.J., 2012. Impactos ecológicos da inundação e seca na vegetação das áreas alagáveis amazônicas. Eventos climáticos Extrem. na Amaz. causas e conseqüências, pp. 405–457.
Pontius, R.G., Millones, M., 2011. Death to Kappa: birth of quantity disagreement and allocation disagreement for accuracy assessment. Int. J. Remote Sens. 32, 4407–4429. https://doi.org/10.1080/01431161.2011.552923.
Pontius, R.G., Santacruz, A., 2014. Quantity, exchange, and shift components of difference in a square contingency table. Int. J. Remote Sens. 35, 7543–7554. https://doi.org/10.1080/2150704X.2014.969814.
Prance, G.T., 1979. Notes on the vegetation of Amazonia III. The terminology of Amazonian forest types subject to inundation. Brittonia 31, 26. https://doi.org/10.2307/2806669.
R Core Team, 2017. R: A Language and Environment for Statistical Computing.
Resende, A.F., Nelson, B.W., Flores, B.M., de Almeida, D.R., 2014. Fire damage in seasonally flooded and upland forests of the Central Amazon. Biotropica 46, 643–646. https://doi.org/10.1111/btp.12153.
Ritter, C.D., McCrate, G., Nilsson, R.H., Fearnside, P.M., Palme, U., Antonelli, A., 2017. Environmental impact assessment in Brazilian Amazonia: challenges and prospects to assess biodiversity. Biol. Conserv. 206, 161–168. https://doi.org/10.1016/j.biocon.2016.12.031.
Schlüter, U.B., Furch, B., 1992. Morphological, anatomical, and physiological investigations on the tolerance to flooding by the tree *Macrolobium acaciifolium*, characteristic of the white- and blackwater inundation forest near Manaus, Amazonas. Amazoniana 12, 51–69.
Schöngart, J., Junk, W.J., 2007. Forecasting the flood-pulse in Central Amazonia by ENSO-indices. J. Hydrol. 335, 124–132. https://doi.org/10.1016/j.jhydrol.2006.11.005.
Schöngart, J., Piedade, M.T.F., Ludwigshausen, S., Horna, V., Worbes, M., 2002. Phenology and stem-growth periodicity of tree species in Amazonian floodplain forests. J. Trop. Ecol. 18, 581–597. https://doi.org/10.1017/S0266467402002389.
Schöngart, J., Piedade, M.T.F., Wittmann, F., Junk, W.J., Worbes, M., 2005. Wood growth patterns of *Macrolobium acaciifolium* (Benth.) Benth. (Fabaceae) in Amazonian black-water and white-water floodplain forests. Oecologia 145, 454–461. https://doi.org/10.1007/s00442-005-0147-8.
Schöngart, J., Wittmann, F., Junk, W.J., Piedade, M.T.F., 2017. Vulnerability of Amazonian floodplains to wildfires differs according to their typologies impeding generalizations. Proc. Natl. Acad. Sci. 114, 201713734. https://doi.org/10.1073/pnas.1713734114.
Shi, Z., Fung, K.B., 1994. A comparison of digital speckle filters. Proc. IGARSS '94 - 1994 - IEEE Int. Geosci. Remote Sens. Symp.. vol. 4, pp. 2129–2133. https://doi.org/10.1109/IGARSS.1994.399671
Silva, T.S.F., Costa, M.P.F., Melack, J.M., Novo, E.M.L.M., 2008. Remote sensing of aquatic vegetation: theory and applications. Environ. Monit. Assess. 140, 131–145. https://doi.org/10.1007/s10661-007-9855-3.
Silva, T.S.F., Costa, M.P., Melack, J.M., 2010. Spatial and temporal variability of macrophyte cover and productivity in the eastern Amazon floodplain: a remote sensing approach. Remote Sens. Environ. 114 (9), 1998–2010.
Silva, T.S.F., Melack, J., Susin, S.A., Ferreira-Ferreira, J., de Almeida Furtado, L.F., 2015. Capturing the dynamics of Amazonian wetlands using synthetic aperture radar: lessons learned and future directions. Remote Sens. Wetl., pp. 455–472 https://doi.org/10.1201/b18210-25\r10.1201/b18210-25
Sioli, H., 1984. The Amazon and Its Main Affluents: Hydrography, Morphology of the River Courses, and River Types. , pp. 127–165 https://doi.org/10.1007/978-94-009-6542-3_5.
Sombroek, W., 2001. Spatial and temporal patterns of Amazon rainfall. AMBIO J. Hum. Environ. 30, 388–396. https://doi.org/10.1579/0044-7447-30.7.388.
Targhetta, N., Kesselmeier, J., Wittmann, F., 2015. Effects of the hydroedaphic gradient on tree species composition and aboveground wood biomass of oligotrophic forest ecosystems in the central Amazon basin. Folia Geobot. 50, 185–205. https://doi.org/10.1007/s12224-015-9225-9.
Tilt, B., 2012. Damming china's angry river: vulnerability in a culturally and biologically diverse watershed. Water, Cultural Diversity, and Global Environmental Change: Emerging Trends, Sustainable Futures?, pp. 367–386 https://doi.org/10.1007/978-94-007-1774-9_26.
Tilt, B., Braun, Y., He, D., 2009. Social impacts of large dam projects: a comparison of international case studies and implications for best practice. J. Environ. Manag. 90, S249–S257. https://doi.org/10.1016/j.jenvman.2008.07.030.
Timpe, K., Kaplan, D., 2017. The changing hydrology of a dammed Amazon. Sci. Adv. 3, 1–14. https://doi.org/10.1126/sciadv.1700611.
Ward, J.V., Stanford, J.A., 1995. Ecosystems and its disruption by flow regulation. Regul. Rivers Res. Manag. 11, 105–119. https://doi.org/10.1002/rrr.3450110109.
Williams, G.P., Wolman, M.G., 1984. Downstream effects of dams on alluvial rivers. U.S. Geol. Surv. Prof. Pap. 1286. https://doi.org/10.1126/science.277.5322.9j.
Williams, E., Antonia, A.D., Antonia, V.D., De Almeida, J.M., Suarez, F., Liebmann, B., Claudia, A., Malhado, M., Dall'Antonia, A., Dall'Antonia, V., 2005. The drought of the century in the Amazon Basin: an analysis of the regional variation of rainfall in South America in 1926. Acta Amaz 35, 231–238.
Wittmann, F., Junk, W.J., 2017. The Wetland Book. , pp. 1–20 https://doi.org/10.1007/978-94-007-6173-5.
Wittmann, F., Schöngart, J., Montero, J.C., Motzer, T., Junk, W.J., Piedade, M.T.F., Queiroz, H.L., Worbes, M., 2006. Tree species composition and diversity gradients in white-water forests across the Amazon Basin. J. Biogeogr. 33, 1334–1347. https://doi.org/10.1111/j.1365-2699.2006.01495.x.
Wittmann, F., Householder, E., Piedade, M.T.F., De Assis, R.L., Schöngart, J., Parolin, P., Junk, W.J., 2013. Habitat specifity, endemism and the neotropical distribution of Amazonian white-water floodplain trees. Ecography 36, 690–707. https://doi.org/10.1111/j.1600-0587.2012.07723.x.
Wittmann, F., Marques, M.C.M., Júnior, G.D., Budke, J.C., Piedade, M.T.F., De Wittmann, A.O., Montero, J.C., De Assis, R.L., Targhetta, N., Parolin, P., Junk, W.J., Householder, J.E., 2017. The Brazilian freshwater wetscape: changes in tree community diversity and composition on climatic and geographic gradients. PLoS One 12, 1–18. https://doi.org/10.1371/journal.pone.0175003.
Woodhouse, I.H., 2017. Introduction to Microwave Remote Sensing. CRC Press.

Yang, D., Li, W., 2013. Soil seed bank and aboveground vegetation along a successional gradient on the shores of an oxbow. Aquat. Bot. https://doi.org/10.1016/j.aquabot.2013.05.004.

Zahar, Y., Ghorbel, A., Albergel, J., 2008. Impacts of large dams on downstream flow conditions of rivers: aggradation and reduction of the Medjerda channel capacity downstream of the Sidi Salem dam (Tunisia). J. Hydrol. 351, 318–330. https://doi.org/10.1016/j.jhydrol.2007.12.019.

Ziegler, A.D., Petney, T.N., Grundy-Warr, C., Andrews, R.H., Baird, I.G., Wasson, R.J., Sithithaworn, P., 2013. Dams and disease triggers on the lower Mekong river. PLoS Negl. Trop. Dis. 7. https://doi.org/10.1371/journal.pntd.0002166.